Deliverable: MOEN/04/04/02/03

Impacts of mean sea level rise based on current state-of-the-art modelling

Debbie Hemming, Jason lowe, Matthew Biginton, Richard Betts, Derrick Ryall

Hadley Centre for Climate Prediction and Research

Delivered from authors: Debbie Hemming	Signature	Date
Scientific content approved by Activity Manager:	Signature	Date
Sent to MOD:	Signature	Date

Contract:

Version Number:

Number of Pages: including cover pages

Table of Contents

Summary

Global average sea level is projected to rise between 0.10m and 0.15m by 2030, 0.18m and 0.30m by 2050, and 0.41m and 0.88m by 2100, depending on the model and scenario used. Projections of people flooded per year globally increase up to 21 million per year by 2030, 55 million per year by 2050, and 370 million per year by 2100. This coincides with estimate of land loss due to submergence of up to 50,000 km^2 of land area lost globally by 2030, 180,000 km^2 by 2050, and 1,130,000 km^2 by 2100.

By combining the estimates of coastal populations and land areas at risk of flooding from sea level rise, it is evident that the key regions of highest risk are concentrated in south and south-east Asia, particularly Bangladesh, India, Pakistan, the Maldives and eastern China. These regions have high floodplain population densities and low sea dikes. Many large river deltas are also at risk, e.g. the Nile, Mississippi, Rio Grande, Rhone and Tigris, largely because these regions are characterised by low lying land prone to high rates of subsidence. Although their population densities are not as high, Indonesia, Africa and the Caribbean are also likely to be high risk regions because they have relatively expansive low lying coastal areas with low dikes.

The uncertainties examined in this study focus on differences in sea level rise projections from a range of climate models and future emissions scenarios. We represent uncertainties by the standard deviation across the range of model and scenario projections. These results show that the dominant uncertainties in sea level rise and associated coastal impacts are caused by differences between climate models. While these uncertainties are usually smaller than the average sea level rise projections, in some locations (across northern Greenland, Arctic islands, southern tip of South America and the Falkland Islands), they are comparable or larger than the average. It is important to remember that these represent only a part of the total uncertainties in the sea level rise and coastal impacts projections, using climate model and emissions scenario information available at the time. They do not account for uncertainties in the coastal data defining population, dike heights and storm characteristics, or how these may evolve over time. As more data becomes available, particularly with the publication of the Intergovernmental Panel on Climate Change's Fourth Assessment Report in 2007, the range of potential sea level increases and their impacts can be quantified more fully.

Detailed summary of key results

Sea level rise projections

- Global average sea level is projected to rise between 0.10m and 0.15m by 2030, 0.18m and 0.30m by 2050, and 0.41m and 0.88m by 2100, depending on the model and emission scenario used.

- After accounting for coastal land uplift and subsidence, global average relative sea level is projected to rise between 0.08m and 0.13m by 2030, 0.17m and 0.29m by 2050, and 0.35m and 0.82m by 2100.

- Thermal expansion of ocean water, as a result of global warming, accounts for the main proportion (~58 %) of absolute sea-level rise, glacial melt is 35 %, Greenland ice sheet increases linearly from about 8 % at the beginning of the 21st century to about 15 % by 2100, and the Antarctic ice sheet decreases from about 2 % at 2000 to about -5 % (i.e. a net gain of ice on land) by 2100.

- By 2030, the regions experiencing the largest relative sea level rises (eastern seaboard of USA, Gulf of Mexico, southern tip of South America and Falkland Islands, Netherlands, and along many of the deltas of large rivers) are projected to show between 0.14m and 0.24m of relative sea level rise, and by 2050, this increases to between 0.24m and 0.35m in the same regions.

- Regions of lowest relative sea level rise tend to be where land uplift is largest, i.e. in high northern latitudes. Large areas of Australia, Indonesia and Japan, and specific localities in South America, Africa, China and New Zealand also show relatively small rises; less than 0.17m by 2050.

- Uncertainties in these projections are dominated by variations between different Global Climate Models. The standard deviation of model projections at each coastal segment is generally less than 0.08m by 2030 and 0.11m by 2050.

Impacts of sea level rise

- The largest populations at risk from sea level rise are concentrated in India, Bangladesh, The Maldives and Java. These regions have high floodplain population densities and low sea dikes.

- Large areas of the coasts of Indonesia, Africa and the Caribbean are likely to be at risk of flooding by sea level rise. These regions have relatively expansive low lying coastal areas with low dikes.

- The largest areas of low lying coastal land (between 5000 km^2 and 40,000 km^2) occur across northern Canada and Alaska, eastern Canada, the Mississippi and Amazon deltas, Netherlands, and eastern Siberia. Other large areas (between 1000 km^2 and 2500 km^2) occur in parts of Northern Europe, Siberia, Indonesia, Australia, New Zealand, Gulf of Mexico, northern Persian Gulf and Bangladesh.

- With high future population growth and greenhouse gas emissions (Special Report on Emissions Scenarios – SRES, A2 scenario), global average Coastal Floodplain Population Density (CFPD) is projected to increase from 0.09 thousand people per km^2 (thou/km^2) in 2000 to 0.2 thou/km^2 by 2100. For the low population growth and emissions scenario (SRES B1), CFPD is projected to increase from 0.09 thou/km^2 in 2000 to nearly 0.12 thou/km^2 by 2050, then reduce to just above 0.09 thou/km^2 by 2100.

- Land Lost due to Submergence (LLS) could account for 50,000 km^2 of land area globally by 2030, 180,000 km^2 by 2050, and 1,130,000 km^2 by 2100.

- The rate of global LLS increases significantly from 2,500 km^2 per year between 1990 and 2040 to 17,500 km^2 per year between 2040 and 2100.

- The largest areas of land loss by 2030 and 2050 are projected to occur across the Arctic Ocean coasts of Canada, Alaska, Siberia and Greenland. This results from large areas of low lying land and low, or no, dikes in these regions.

- In more populated regions, land losses of between 2,500 km^2 and 5,000 km^2 per year are projected along the coast of Pakistan, south-eastern Indonesia and eastern Africa from Kenya south to Mozambique and Sri Lanka.

- For the high population growth and emissions scenario, SRES A2, the number of People Flooded per year (PF) globally is projected to increase to 21 million per year by 2030, 55 million per year by 2050, and 370 million per year by 2100. For the low population growth and emissions scenario, SRES B1, PF projections are 18 million per year by 2030, 42 million by 2050, and 165 million by 2100.

- As was noted for LLS, after 2040 the rate of rise in the global number of PF per year increases from ~10 million per decade for both future population growth scenarios, to ~60 million per decade for the SRES A2 scenario and 25 million per decade for the SRES B1 scenario.

- The most vulnerable populations to coastal flooding from sea level rise are located in south and south-east Asia, particularly Bangladesh, India, Pakistan, eastern China, and southern Indonesia. Other susceptible regions are also noted along the east coast of Africa, southern tip of Chile and the Nile delta. By 2050, the populations most at risk are in the Bay of Bengal, where up to 2.5 million PF per year are estimated.

1. Introduction

Almost half of the global population lives in coastal zones, and in many countries the coastal population has been growing at double the national rate (IPCC, 1998). In these locations, the high-density population centres and areas of intensive agriculture (often located on coastal deltas) are particularly vulnerable to the impacts of sea level rise.

Sea level changes are an important response to climate change. Since the last glacial maximum, about 20,000 years ago, relative sea level has risen by over 120m in some regions, as a result of the melting of land-based ice into the oceans. From 15,000 to 6,000 years ago the average rate of global sea level rise was 10 mm/year. This slowed to between 0.1 and 0.2 mm/year in the last 3,000 years, and tidal gauge information during the 20th century indicates that no significant change in this rate has occurred over the last century. Projections of future sea level rise for the 21st century suggest that this rate of rise could increase by up to 4 times, and will continue to rise for several centuries because of the long ocean response time (IPCC, 2001).

In this report, we assess the impacts of global sea level rise on coastal regions using sea level rise projections from an ensemble of Global Climate Models (GCMs) and future emissions scenarios from the Special Report on Emissions Scenarios (SRES). We utilise the Dynamic and Interactive Vulnerability Assessment (DIVA) model to estimate the regional patterns of sea level rise relative to vertical land movements. Key coastal information available in the DIVA model, such as population and floodplain area, are also used to assess the major regions at risk from sea level rise, and estimate the potential populations and areas of land flooded under future sea level rise projections. Throughout this report, the results are discussed with particular focus on the time periods 2030 and 2050 as these were specified as the periods of most interest for MOD planning. To provide additional context, some reference is also made to results for 2100.

2. Methodology

2.1. Calculation of absolute sea level rise

Absolute sea level rise refers to volumetric increases in sea level. This is composed of two main parts; 1) warming of the ocean which expands the existing water volume, and 2) melting of land-based ice which adds water to the ocean.

Projections of future absolute sea level rise vary depending on the Global Climate Model (GCM) used in the simulation, and the assumptions made regarding future greenhouse gas emissions. To understand this uncertainty we use an ensemble of twenty future sea level rise projections, produced by forcing five different GCMs with four distinctly different future emissions and socio-economic scenarios taken from the Special Report on Emissions Scenarios (SRES) (see IPCC, 2000 for details). Table 1 shows details of the GCMs used.

Table 1. GCMs and SRES scenarios used to generate absolute sea level rise data.

Model	Spatial Resolution	Host Institute	Reference
CSIRO Mk2	5.6º lat 3.2º long	Commonwealth Scientific & Industrial Research Organisation, Australia.	Hirst et al, 1996
ECHAM4	2.8º lat 2.8º long	Max Planck Institute for Meteorology, Hamburg. Germany.	Roeckner et al, 1996
GFDL R15	7.5º lat 4.5º long	Geophysical Fluid Dynamics Laboratory, Princeton. USA	Haywood et al, 1997
HadCM2	3.75º lat 2.5º long	Hadley Centre, UK Met Office	Mitchell & Johns, 1997
HadCM3	2.5º lat 3.75º long	Hadley Centre, UK Met Office	Gordon et al, 2000

The four SRES scenarios used in this report are known as A1FI, A2, B1 and B2. Major features of these scenarios are:

A1FI describes a future world of very rapid economic growth, intensive fossil fuel use and rapid introduction of new and more efficient technologies. Global population peaks in mid-century and declines thereafter. Throughout this storyline there is a substantial reduction in the regional differences in per capita income.

A2 describes a very heterogeneous world. There is an underlying theme of self-reliance and preservation of local identities. Population increases continuously throughout the 21st century, and economic development and technological change are more fragmented and slower than in other storylines.

B1 describes a convergent world where global population remains the same until mid-century then declines as in A1FI. Economic changes occur rapidly towards a service and information structure in which resource-efficient technologies become more important.

B2 describes a world of local solutions to economic, social and environmental sustainability. Population increases continuously throughout this storyline, but at a lower rate than for A2. Economic development and technological changes are intermediate compared to the other storylines.

Global patterns of absolute sea level rise between 1990 and 2100 for each model and SRES scenario were calculated (Equation 1) by combining a) the global mean trends in sea level for each model and SRES scenario, and b) existing spatial patterns of absolute sea level changes that had been generated for earlier studies using the 'IS92' emissions scenario (see IPCC, 2000).

$$P_m(SRES,t) = \left[P(IS92,t) \big/ \overline{P(IS92,t)} \times X(SRES,t) \right] + I(SRES,t) \qquad (1)$$

where,

$P_m(SRES,t)$ is the pattern of sea level rise forced by a particular GCM, m, and SRES scenario at time t.

P(IS92,t) is the pattern of sea level rise forced by the IS92 scenario at time t.

$\overline{P(IS92,t)}$ is the global average sea level rise forced by the IS92 scenario at time t.

X(SRES,t) is the thermal expansion component for the SRES scenario at time t.

I(SRES,t) is the ice components (glaciers, and Greenland and Antarctic ice sheets) for the SRES scenario at time t.

2.2. Calculation of relative sea level rise

To assess the impacts of sea level rise it is necessary to understand the spatial distribution of relative sea level rise, which takes account of the vertical movements of coastal land. In regions where land is subsiding, relative sea level rise will be greater than absolute, and the potential impacts of sea level rise on coastal regions will be accentuated, and *vice versa*.

Global patterns of relative sea level rise are estimated for the period 2000 to 2100 by combining the spatial estimates of absolute sea level rise, for each of the five global climate models and four SRES scenarios (see section 2.1.), with high-resolution coastal data of vertical land uplift and subsidence. This is done using the Dynamic and Interactive Vulnerability Assessment model, DIVA (Hinkel, 2005).

The dataset of coastal land movements is shown in Figure 1. It is composed of 12,148 coastline segments (average length 70km), each of which is assumed to exhibit homogeneous sea level rise vulnerabilities (Hinkel, 2005). These movements can occur as a result of a) 'glacio-isostatic' adjustments, as interpolated from the geophysical model of Peltier (2000), which result mainly from the unloading (by melting) of ice sheets after the last glaciation, and/or b) subsidence of deltas, as defined by McGill (1958), where a uniform background rate of 2 mm/year is assumed. Other changes in land heights, such as human-induced subsidence as a result of groundwater extraction, are not considered.

It is clear from Figure 1 that the coastal areas experiencing the fastest land uplift (coastline highlighted in green) are distributed across the high latitudes, particularly NE Canada, NW

Siberia, and Scandinavia, as a result of glacio-isostatic unloading. At the other extreme, many of the regions experiencing the most rapid subsidence (coastline highlighted in red, brown and black) are at river deltas, including the Mississippi, Rio Grande, Rhone, Nile and Tigris (see annotations on Figure 1). The Gulf of Mexico coast in general is particularly vulnerable to subsidence.

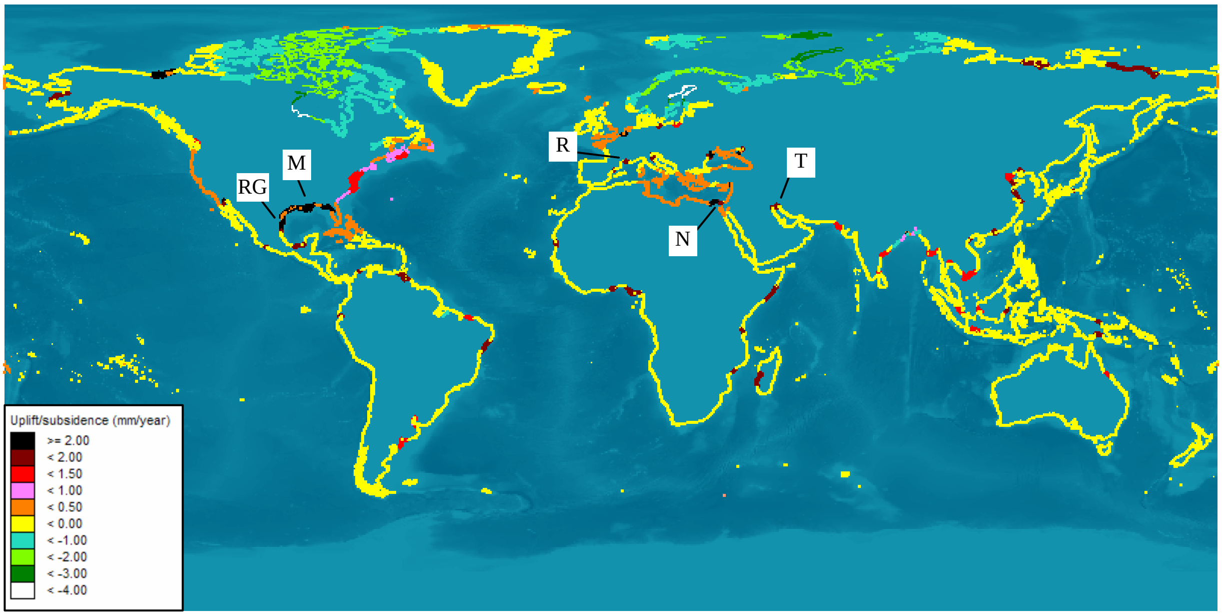

Figure 1. Rates (mm/year) of coastal land uplift (negative values) and subsidence (positive values) in 1990. Annotations show the locations of major river deltas experiencing the most rapid subsidence; Mississippi (M), Rio Grande (RG), Rhone (R), Nile (N) and Tigris (T).

2.3. Estimation of areas at risk and potential impacts of sea level rise

Relative sea-level rise will have multiple direct and indirect impacts on coastal regions. In this report, we use the DIVA model, which incorporates information on the physical, ecological and socio-economic characteristics of the world's coastal regions (excluding Antarctica), to identify key regions at risk from sea level rise, and estimate the direct impacts of sea level rise on inundation of coastal populations and land areas. We also examine uncertainties in these estimates that relate to the variability among models and scenarios.

The DIVA model integrates the relative sea level rise projections (see section 2.2) with detailed maps of surface elevation, coastal dike heights and estimates of coastal population. Population is estimated using the IMAGE2.2 17-region implementation of the SRES scenarios (IMAGE Team, 2002; Nakicenovic and Swart, 2001), where growth rates are assumed to be homogeneous throughout all countries in a region. Coastal population growth rates are assumed to be double the national average, which is in line with current trends. It is also assumed that coastal dike heights are kept constant at their 1990 levels (see section 4.2.), and the frequency of storms that drive surges remains constant at the 1990 levels.

While we examine uncertainties that arise as a result of differences between models and future emissions scenarios, it is important to note that the coastal parameters used in the DIVA model also contain uncertainties that are not assessed in this study. In particular, the accuracy of the DIVA results will be sensitive to the specification of dike heights and storm characteristics. Furthermore, no attempt is made in this study to quantify the indirect impacts of sea level rise on factors such as water supply, human health, agriculture, and migration, although, in many regions, such impacts are likely to be larger and more wide-ranging than the direct impacts.

The risk and impacts of relative sea level rise on coastal populations and land area are analysed and presented at the scale of coastal administrative regions (see Figure 2). There are two main reasons for this; 1) many of the datasets used by DIVA, including population and coastal floodplain area, are based on single average values per administrative regions, and 2) the policy implications of relative sea level rise are generally considered at the scale of administrative region or larger.

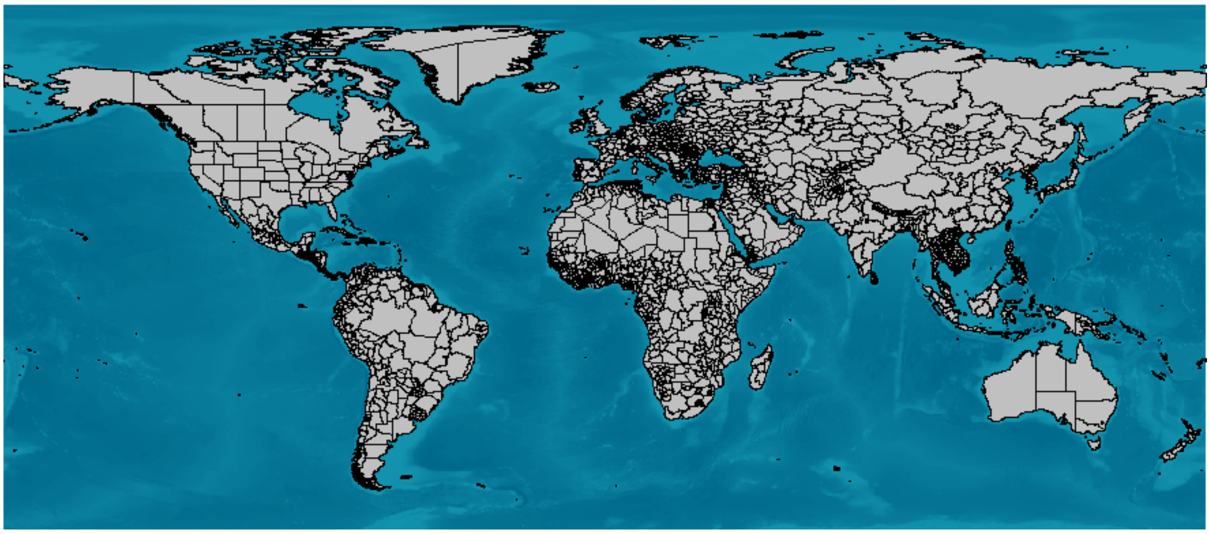

Figure 2. Administrative units used in DIVA model.

3. Future sea level rise projections and uncertainties

3.1. Absolute sea level rise

Figure 3 and Table 2 show the projected changes in absolute sea level between 1990 and 2100 for each of the five GCMs and four SRES scenarios, and for the average of all models and scenarios. The average absolute sea level rise of all models and scenarios is 0.12m by 2030, 0.23m by 2050 and 0.61m by 2100 (Figure 3f & Table 2).

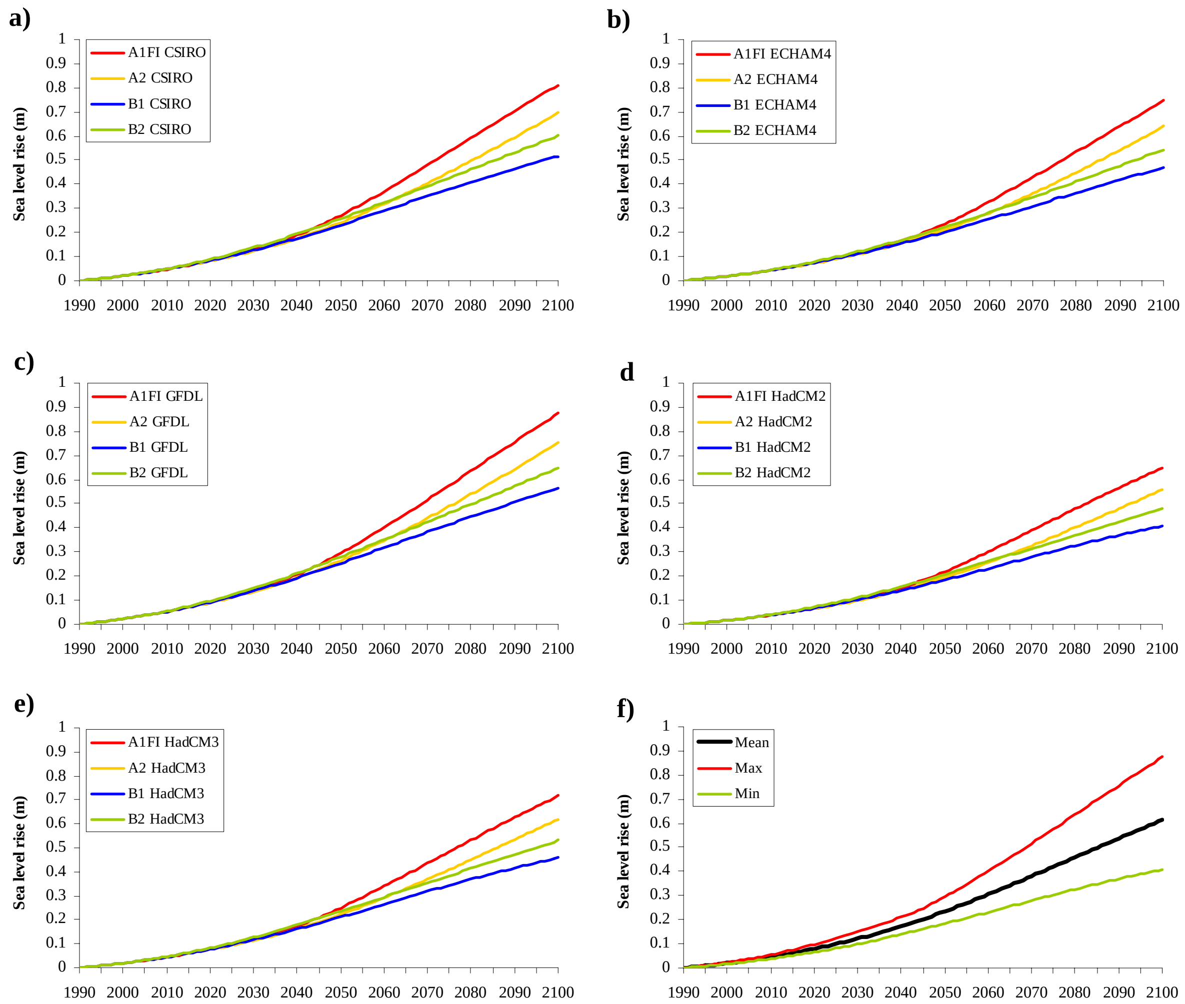

Figure 3. Global average absolute sea level rise for five GCM's; a) CSIRO Mk2, b) ECHAM4, c) GFDL R15, d) HadCM2, e) HadCM3, and four SRES scenarios (A1FI, A2, B1, B2). Figure f) shows the average, maximum and minimum absolute sea level rise values across all models and scenarios.

Depending on the GCM and scenario, global mean absolute sea level is projected to rise between 0.10m and 0.15m by 2030, 0.18m and 0.30m by 2050, and 0.41m and 0.88m by 2100. These uncertainties between the different models and scenarios are related to variations in the specific climate changes simulated. The A1FI and A2 scenarios show the highest increases in sea level for all models because these scenarios result in the largest rises in CO_2 concentrations and therefore highest global average temperatures. Similarly, the B1 and B2 scenarios result in the lowest emissions and smallest global sea level increases in all models.

Table 2. Global average absolute sea level rise, relative to 1990 values, for each model and scenario at each decade. The last two rows show the average (Average) and standard deviation (*SD*) of all models and scenarios. Values are in meters.

		Global average absolute sea level rise relative to 1990 (m)										
Model	**Scenario**	**2000**	**2010**	**2020**	**2030**	**2040**	**2050**	**2060**	**2070**	**2080**	**2090**	**2100**
CSIRO Mk2	**A1FI**	0.02	0.05	0.08	0.13	0.19	0.27	0.37	0.48	0.59	0.70	0.81
	A2	0.02	0.05	0.08	0.12	0.18	0.24	0.32	0.40	0.50	0.59	0.70
	B1	0.02	0.05	0.08	0.13	0.18	0.23	0.29	0.35	0.41	0.47	0.52
	B2	0.02	0.05	0.09	0.14	0.19	0.26	0.32	0.39	0.46	0.53	0.60
ECHAM4	**A1FI**	0.02	0.04	0.07	0.11	0.17	0.24	0.33	0.43	0.53	0.64	0.75
	A2	0.02	0.04	0.07	0.11	0.16	0.21	0.28	0.36	0.45	0.54	0.64
	B1	0.02	0.04	0.07	0.11	0.15	0.20	0.25	0.31	0.37	0.42	0.47
	B2	0.02	0.04	0.08	0.12	0.17	0.22	0.28	0.35	0.41	0.48	0.54
GFDL R15	**A1FI**	0.02	0.05	0.09	0.14	0.21	0.30	0.40	0.52	0.64	0.76	0.88
	A2	0.02	0.05	0.09	0.14	0.19	0.27	0.35	0.44	0.54	0.64	0.75
	B1	0.02	0.05	0.09	0.14	0.19	0.25	0.32	0.38	0.45	0.51	0.56
	B2	0.02	0.05	0.10	0.15	0.21	0.28	0.35	0.42	0.50	0.57	0.65
HadCM2	**A1FI**	0.02	0.04	0.07	0.10	0.15	0.22	0.30	0.39	0.48	0.57	0.65
	A2	0.02	0.04	0.07	0.10	0.14	0.19	0.26	0.33	0.40	0.48	0.56
	B1	0.02	0.04	0.07	0.10	0.14	0.18	0.23	0.28	0.33	0.37	0.41
	B2	0.02	0.04	0.07	0.11	0.16	0.21	0.26	0.32	0.37	0.42	0.48
HadCM3	**A1FI**	0.02	0.04	0.08	0.12	0.17	0.25	0.34	0.44	0.53	0.63	0.72
	A2	0.02	0.04	0.08	0.11	0.16	0.22	0.29	0.37	0.45	0.53	0.62
	B1	0.02	0.04	0.08	0.12	0.16	0.21	0.27	0.32	0.37	0.42	0.46
	B2	0.02	0.05	0.08	0.13	0.18	0.24	0.29	0.35	0.41	0.47	0.53
Average		**0.02**	**0.05**	**0.08**	**0.12**	**0.17**	**0.23**	**0.31**	**0.38**	**0.46**	**0.54**	**0.61**
SD		***0.002***	***0.005***	***0.009***	***0.014***	***0.020***	***0.030***	***0.043***	***0.060***	***0.080***	***0.102***	***0.125***

The cumulative and percentage contributions of each of the main sources of absolute sea level rise to the average absolute sea level rise of all models and scenarios is shown in Figures 4 and 5.

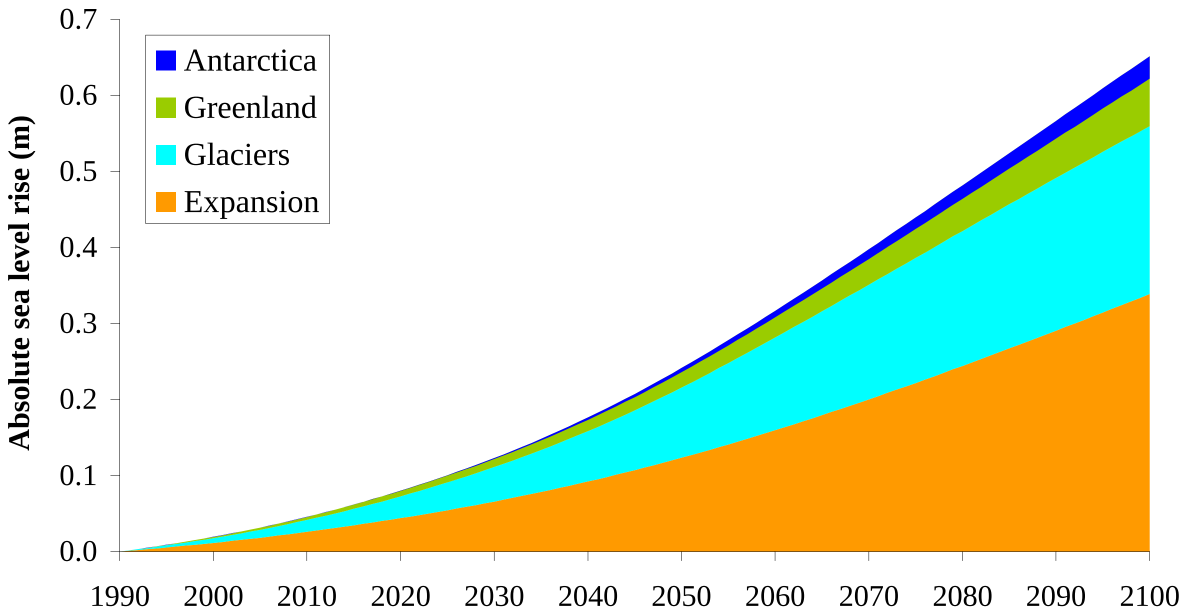

Figure 4. Model and scenario average contributions to absolute sea level rise from thermal expansion of ocean water (orange), glacier melt (light blue), and melt from the Greenland (green) and Antarctic (dark blue) ice sheets.

Thermal expansion of ocean water, as a result of global warming, accounts for the main proportion (~58 %) of total absolute sea level rise, and this remains relatively constant throughout the 21st century (Figure 5). The contribution from glacial melt is also relatively constant at about 35 % of total sea level rise. In comparison, the contribution from the Greenland ice sheet increases linearly from about 8 % at the beginning of the 21st century to about 15 % by 2100, and the contribution from the Antarctic ice sheet decreases from about 2 % at 2000 to about -5 % by 2100, i.e. a net gain of ice on land. Increasing precipitation over the East Antarctic ice sheet is the likely cause of this projected net accumulation of water on Antarctica in the second half of the 21st century.

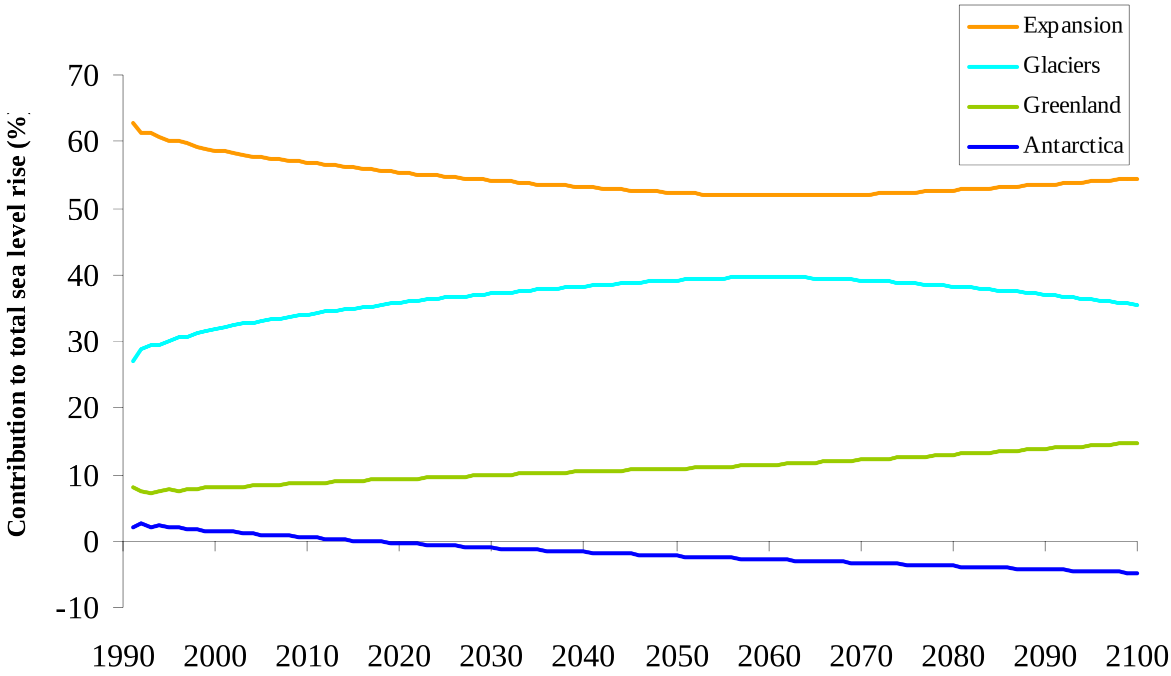

Figure 5. Percentage contributions to total mean sea level rise from thermal expansion of ocean water (orange), glacier melt (light blue), and melt from the Greenland (green) and Antarctic (dark blue) ice sheets.

3.2. Relative sea level rise

To assess the risks and impacts of coastal regions to sea level rise, it is necessary to estimate the relative sea level rise (see section 2.2.). After accounting for coastal land uplift and subsidence, the global average relative sea level for all models and scenarios is projected to rise (relative to 1990 levels) by 0.1m by 2030, 0.22m by 2050 and 0.68m by 2100 (Figure 6a and 7a). These values are slightly lower than those for absolute sea level rise because the global average movement of coastal land is uplifting, as a result of the dominant influence of isostatic rebound in high northern regions (see Figure 1).

As land uplift and subsidence rates are identical for all models and scenarios, the uncertainties in relative sea level rise that relate to the choice of model or future emissions scenario are the same as for absolute sea level rise (see Figure 3 and Table 2). Consequently, the range of relative sea level rise projections across all models and scenarios is between 0.08m and 0.13m by 2030, 0.17m and 0.29m by 2050, and 0.35m and 0.82m by 2100.

Global average trends in sea level rise mask large spatial variability that results from uneven global patterns of climate change, which influence the rates of thermal expansion of the oceans and melting or accumulation of glaciers and ice sheets. Furthermore, spatial differences in uplift and subsidence affect the relative sea level rise in any particular location.

Figures 6 and 7 compare the global average trend in relative sea level rise (Figures 6a and 7a) with spatial variations in the relative sea level rise of all models and scenarios at 2030 and 2050 (Figure 6b and 7b). These figures also indicate the spatial uncertainties in these projections that result from differences between models (Figures 6c and 7c) and scenarios (Figure 6d and 7d).

Relative sea level rise is projected to be largest along the eastern seaboard of USA, Gulf of Mexico, southern tip of South America and Falkland Islands, Netherlands, and at many of the deltas of large rivers, including the Mississippi, Rio Grande, Rhone, Nile, Euphrates/Tigris and Niger. By 2030, these worst affected areas are projected to experience between 0.14m and 0.24m of relative sea level rise (Figure 6b), and by 2050, this has increased to between 0.24m and 0.35m in the same regions (Figure 7b).

Most of the regions with the lowest projections of relative sea level rise occur in high northern latitudes, where land uplift is largest, although large areas of Australia, Indonesia and Japan, and specific localities in South America, Africa, China and New Zealand also show relatively small increases of less than 0.17m by 2050.

Uncertainties in the relative sea level rise projections are dominated by the variations between different models (Figures 6c and 7c). The standard deviation of model projections at each coastal segment is generally less than 0.08m at 2030 and 0.11m at 2050. In a few regions these model uncertainties are larger. For example, in northern Greenland by 2030 the standard deviation of sea level rise across all models is between 0.08m and 0.11m, which is larger than the projected average sea level rise of between 0.05m and 0.08m in this region. The largest model uncertainties by 2050 are between 0.11m and 0.14m, and these occur across northern Greenland, the Svalbard Islands in the Arctic, and the southern tip of South America and Falkland Islands. The uncertainties in relative sea level rise between different emissions scenarios (Figures 6d and 7d) are negligible (less than 0.04m) both by 2030 and 2050.

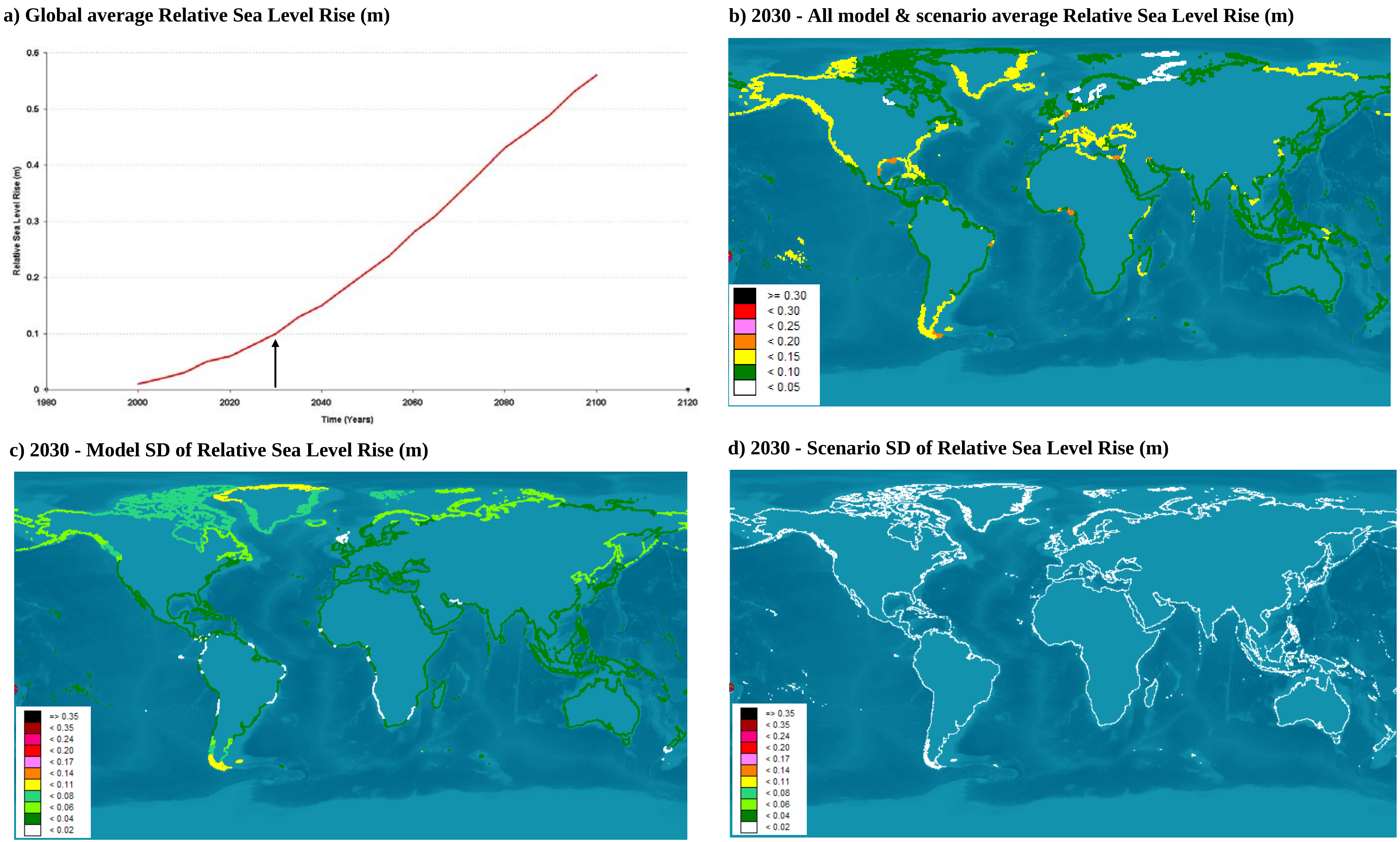

Figure 6. Relative Sea Level Rise (m) for a) 2000 to 2100 global average time series, b) 2030 average for all models and scenarios, & c) 2030 standard deviation across all models, & d) 2030 standard deviation across all scenarios.

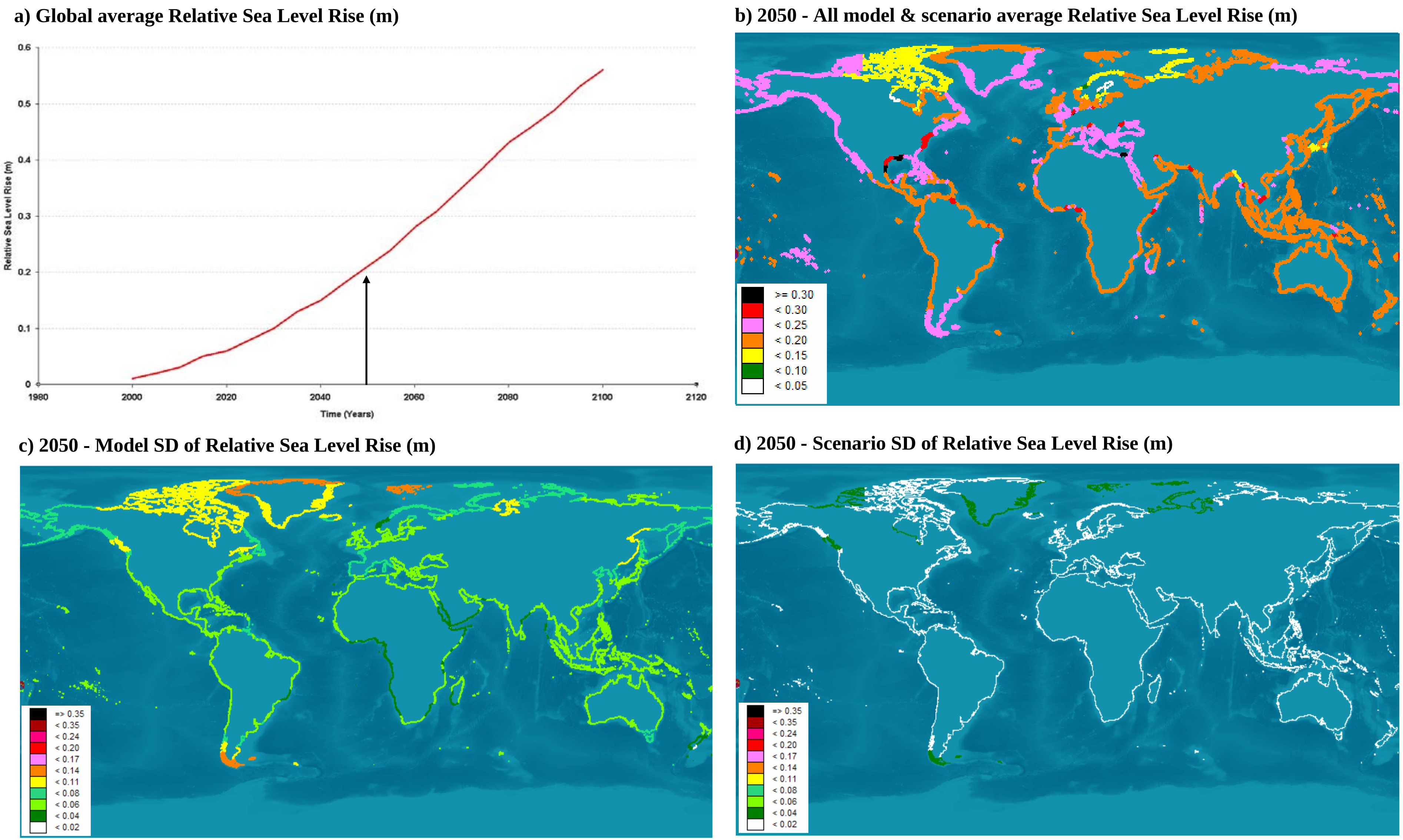

Figure 7. Relative Sea Level Rise (m) for a) 2000 to 2100 global average time series, b) 2050 average for all models and scenarios, & c) 2050 standard deviation across all models, & d) 2050 standard deviation across all scenarios.

4. Impacts of sea level rise

4.1. Land and people at risk

Here, we assess the vulnerability of coastal regions to relative sea level rise by comparing the areas of low lying coastal land, current coastal defences (sea dike heights), and future projections of the population density on coastal floodplains. Regions that exhibit large areas of low lying coastal land, little or low sea dikes and high floodplain populations are considered most at risk to sea level rise.

Figure 8 shows the areas of coastal land that are located less than 1m above average sea level. The largest areas of low-lying coastal land (between 5000 km^2 and 40,000 km^2) occur across northern Canada and Alaska, eastern Canada, the Mississippi and Amazon deltas, Netherlands, and eastern Siberia. Other large areas (between 1000 km^2 and 2500 km^2) occur in parts of Northern Europe, Siberia, Indonesia, Australia, New Zealand, Gulf of Mexico, northern Persian Gulf and Bangladesh.

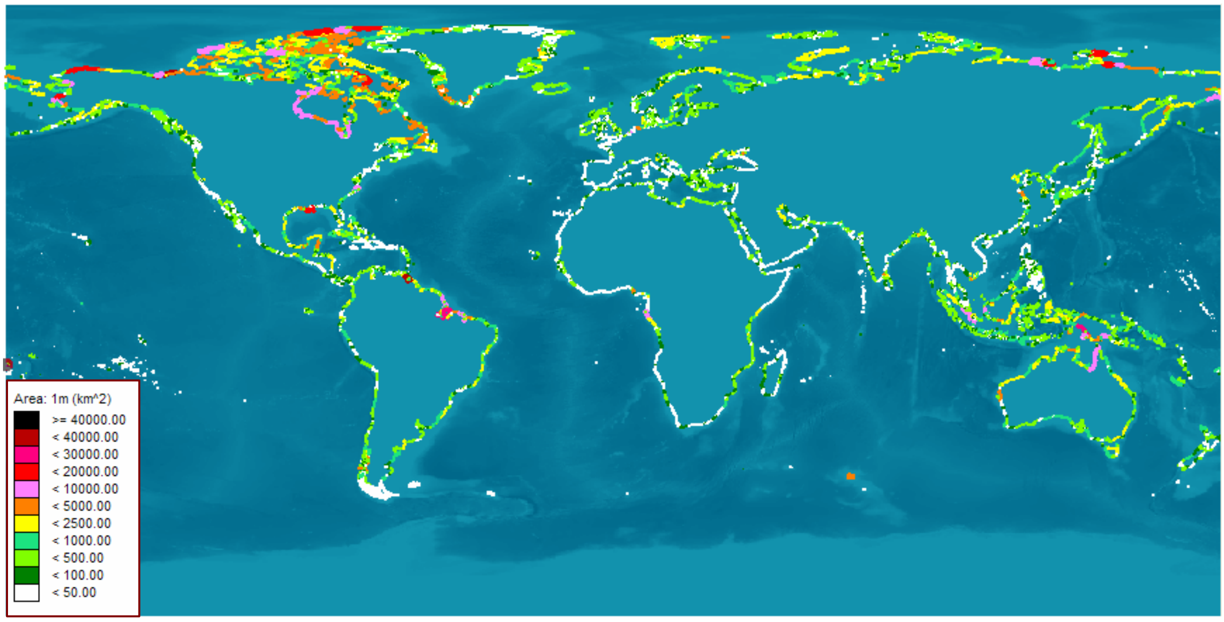

Figure 8. Coastal land areas less than 1m height above average sea level in 1990.

Sea dikes are not the only form of coastal defence. However, global information on the height of current sea dikes provides an indication of the level of protection that currently exists in different regions. Figure 9 shows the current knowledge of the height of sea dikes in 1990. The vast majority of coastal regions around the globe have dike heights below 2.0m. Along with sizeable areas in the high Arctic, large areas of coastline in Africa, Indonesia and the Caribbean accommodate the lowest dike heights of less than 1.0m.

Regions with the highest dikes, between 7.0m to 13.5m, are clearly focused in developed countries, e.g. in north-west Europe (particularly the Netherlands and Belgium), north-west and east North America, south-east South America, Korea, Japan, and north and north-west Australia.

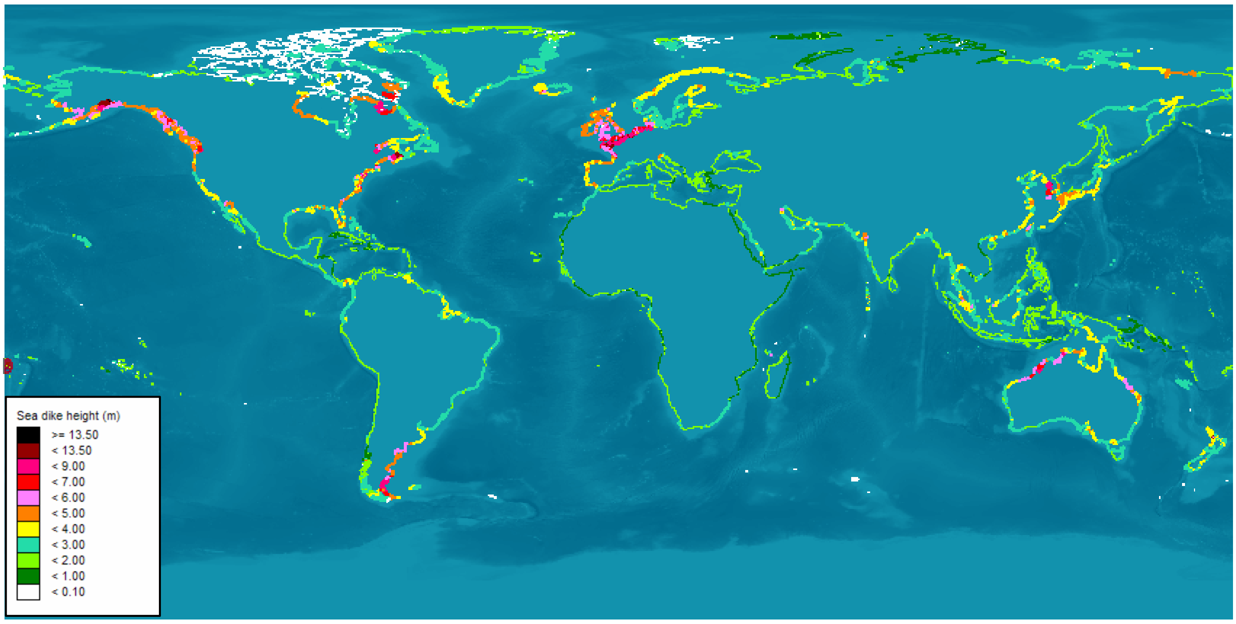

Figure 9. Sea dike heights (m) in 1990.

Coastal floodplain population density (CFPD) provides an indication of the population in different regions that are potentially at risk from coastal flooding. In this case, floodplain is defined as the area flooded by a storm surge event that has a 1 in 1000 year frequency. As well as uncertainties in climate changes that relate to the choice of GCM and emissions scenario (see section 2.1.), future CFPD changes are very dependent on the future projections of coastal populations. These additional uncertainties are examined by comparing the global average CFPD projections for the 21st century calculated with the high (A2) and low (B1) population scenarios (Figure 10a).

With the high, A2, scenario of coastal population change (red line in Figure 10a), global average CFPD is projected to increase from 0.09 thousand people per km^2 (thou/km^2) in 2000 to 0.2 thou/km^2 by 2100. The rate of rise is reasonably constant at 0.011 thou/km^2 per decade. In comparison, assuming the low coastal population rise scenario (B1) (blue line in Figure 10a), CFPD is projected to increase from 0.09 thou/km^2 in 2000 to nearly 0.12 thou/km^2 by 2050, then reduce to just above 0.09 thou/km^2 by 2100.

To examine the spatial projections of CFPD we have used the higher (A2) scenario of coastal population. In general, the spatial changes projected with the B1 coastal population scenario (not shown here) follow similar patterns, but with reduced magnitudes.

The highest CFPD's for the A2 population scenario are between 1 thou/km^2 and 5 thou/km^2 by 2050 (Figure 10b and c). They occur in Bangladesh, along the west coast of India, in southern Japan, the Nile delta, and at some large coastal cities, e.g. Dakar and Singapore. The magnitude and spatial distribution of CFPD shows little variation between 2030 and 2050, or between the A2 and B1 scenarios of coastal population (Figures not shown). The uncertainties in the projections are dominated by differences in population between scenarios.

a) Global average Coastal Floodplain Population Density (thou/km^2)

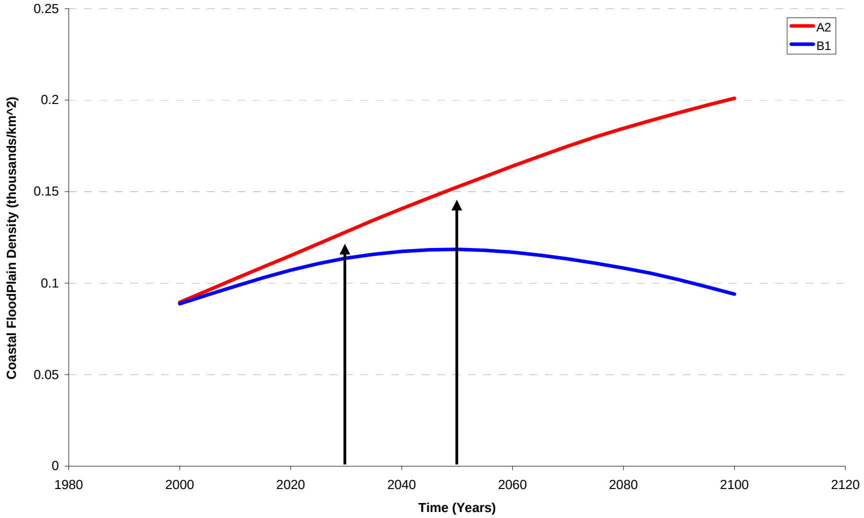

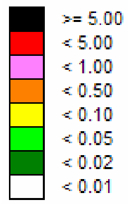

b) 2030 – A2 Coastal Floodplain Population Density (thou/km^2), A2 population

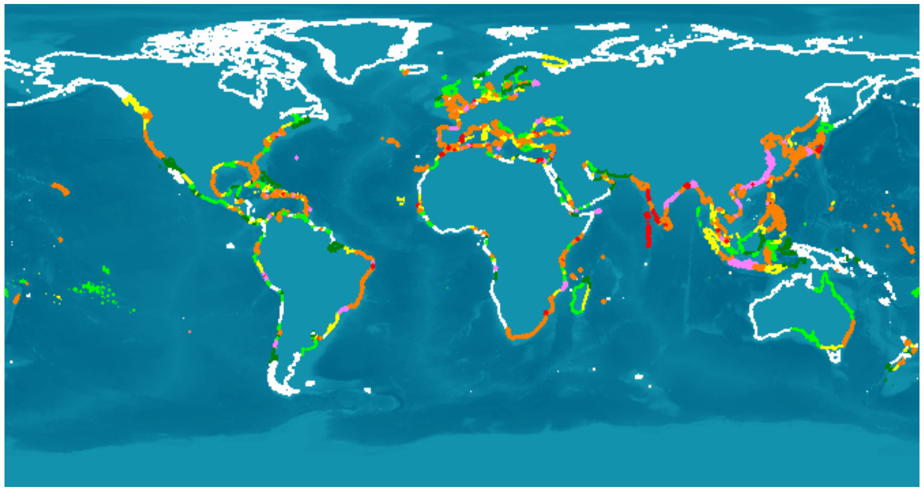

c) 2050 – A2 Coastal Floodplain Population Density (thou/km^2), A2 population

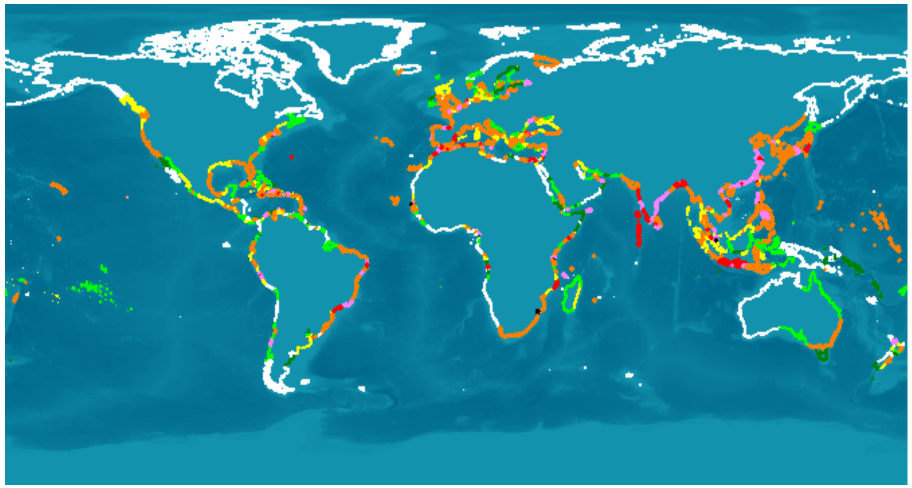

Figure 10. Coastal floodplain population density (thousands/km^2) for a) 2000 to 2100 global average time series with population change according to the A2 and B1 SRES scenarios, b) 2030 average for all models and scenarios with A2 population, & c) 2050 average for all models and scenarios with A2 population.

4.2. Land lost due to submergence (LLS)

Figures 11 and 12 show the estimated land area lost globally, and regionally at 2030 and 2050 (relative to 1990), as a result of submergence caused by sea level rise. These projections indicate that close to 50,000 km^2 of land area could be lost globally by 2030, 180,000 km^2 by 2050, and 1,130,000 km^2 by 2100 (Figure 11a).

The rate of global land area lost increases significantly from 2,500 km^2 per year between 1990 and 2040 to 17,500 km^2 per year between 2040 and 2100. This increase in rate after 2040 is not related with a change in the rate of relative sea level rise (see Figure 6a). Instead, after 2040 a larger area of coastal land is susceptible to submergence both as a result of the nature of the coastal topography in areas without coastal defences, and because increasing numbers of dikes would be breached by rising sea levels after this time. This estimate is based on dike heights remaining constant at current levels. If coastal defences are improved into the future, land lost could be reduced greatly, depending on the location and nature of the defence.

Figures 11b and 12b show the spatial distribution of estimated LLS by 2030 and 2050, and the two lower figures (c and d) provide associated indications of the spatial uncertainties across the range of models and scenarios. The regions with the largest areas of LLS by 2030 and 2050 are northern Canada, Alaska, Siberia and Greenland. This results both from relatively high sea level rise (Figure 6 and 7), and low (or no) dikes (Figure 9) in these regions. In more populated regions, land losses of between 2,500 km^2 and 5,000 km^2 per year are projected along the coast of Pakistan, south-east Indonesia, and east Africa (from Kenya south to Mozambique and Sri Lanka).

Both the model and scenario uncertainties are similar for the projections of LLS (Figures 11 and 12 c and d). The largest uncertainties coincide with the largest land loss regions, and the model and scenario standard deviations are generally comparable in magnitude with the average land loss. By 2050, the largest uncertainties result from differences between climate models, which increase significantly between 2030 and 2050 across Indonesia.

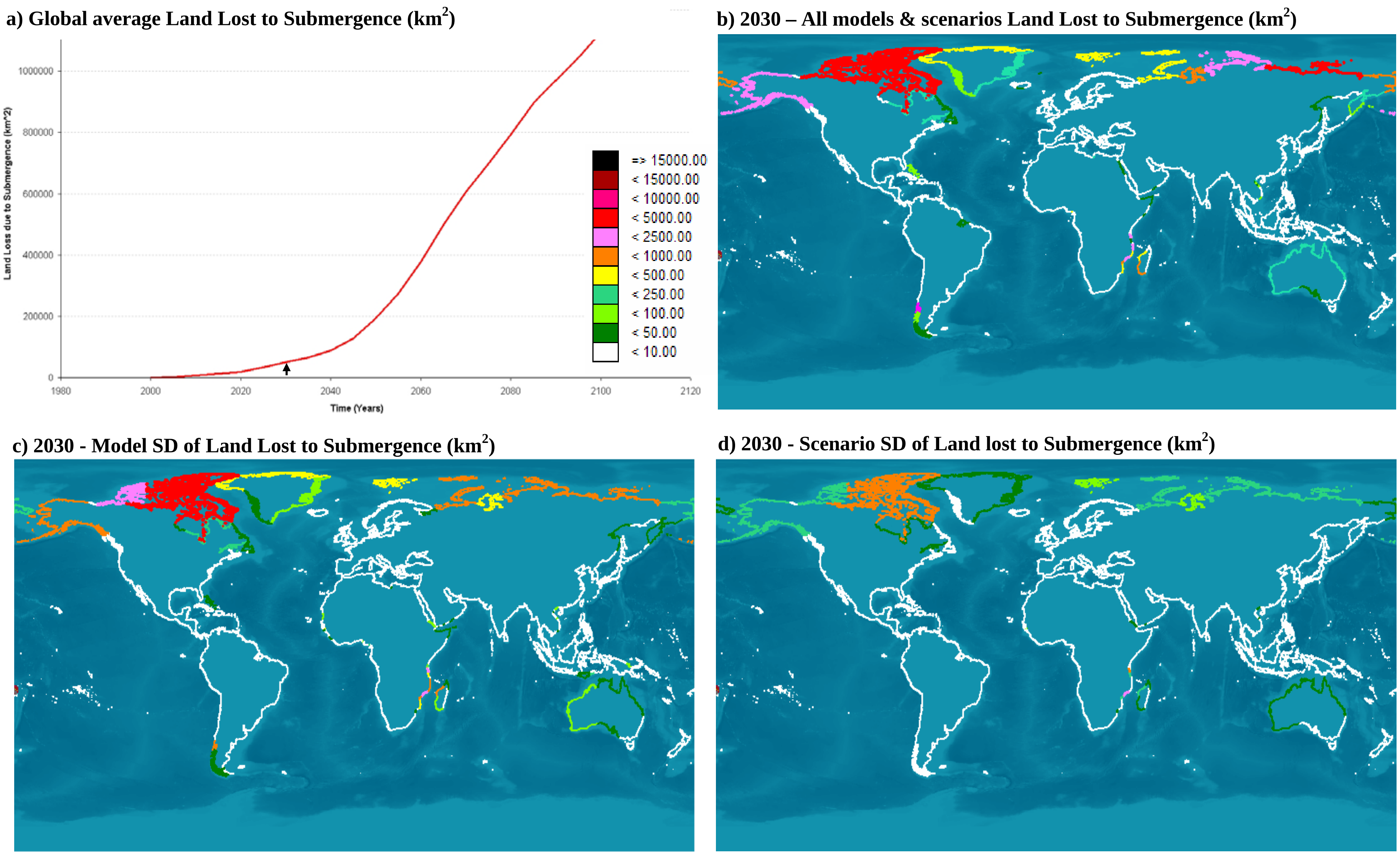

Figure 11. Land Lost due to Submergence (km²) for a) 2000 to 2100 global average time series, b) 2030 average for all models and scenarios, & c) 2030 standard deviation across all models, & d) 2030 standard deviation across all scenarios.

a) Global average Land Lost to Submergence (km^2)

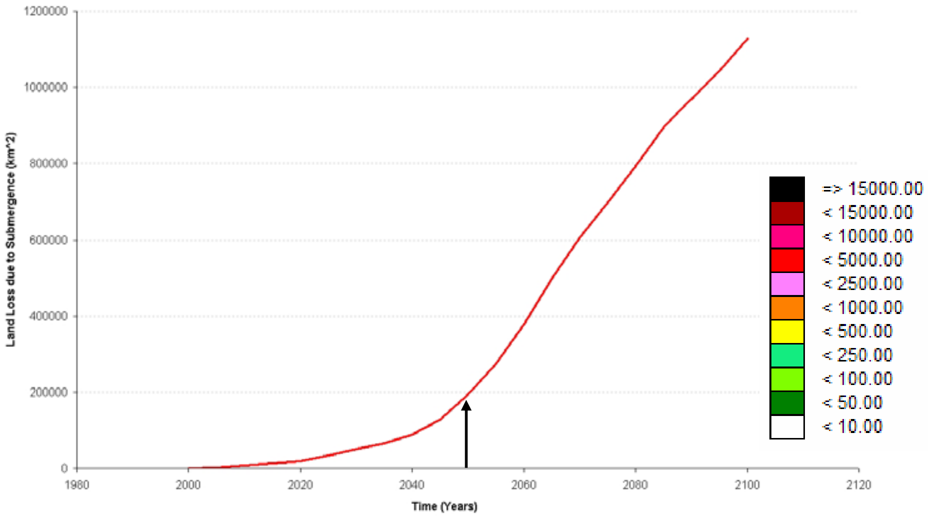

b) 2050 – All models & scenarios Land Lost to Submergence (km^2)

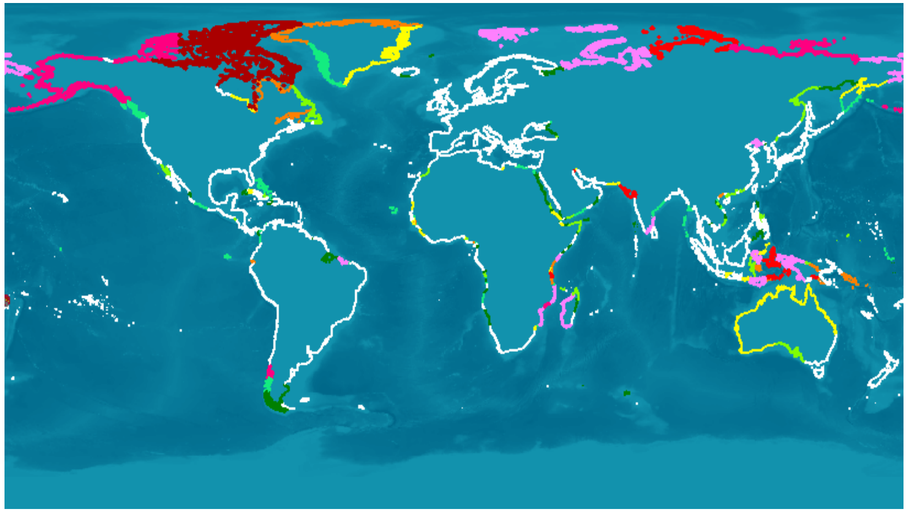

c) 2050 - Model SD of Land Lost to Submergence (km^2)

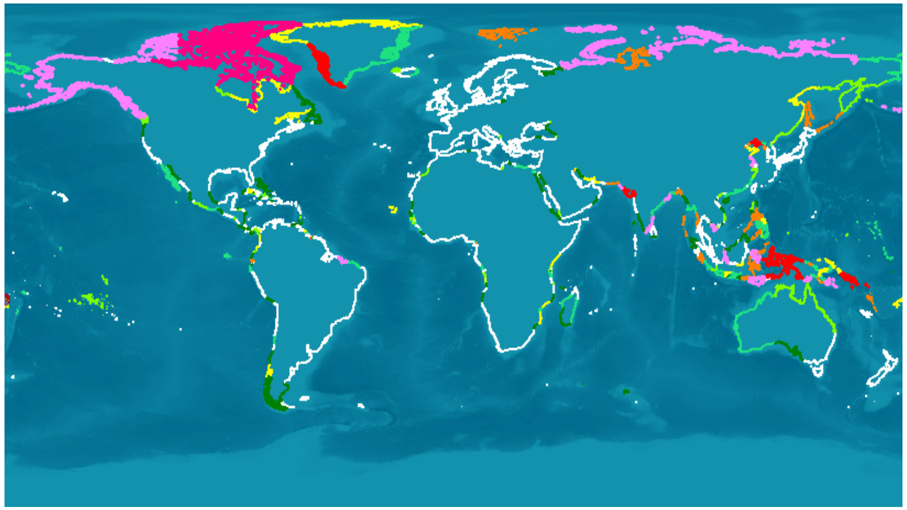

d) 2050 - Scenario SD of Land lost to Submergence (km^2)

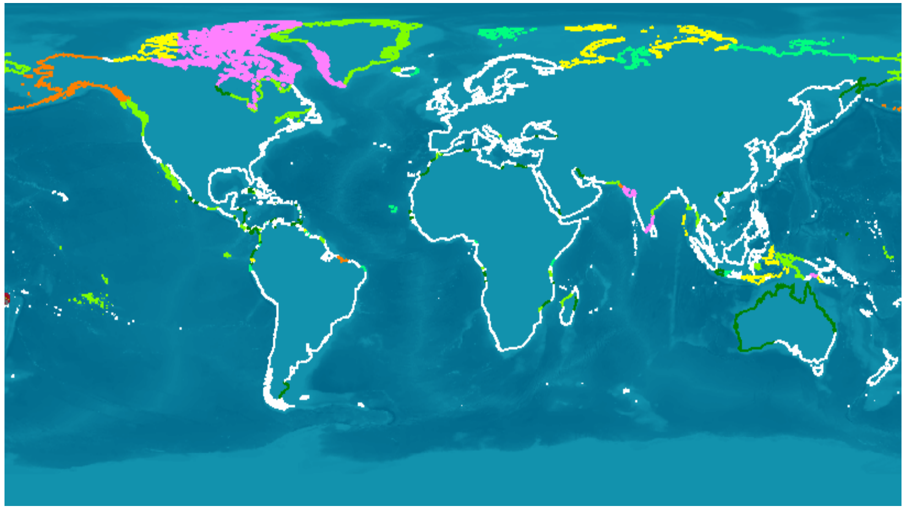

Figure 12. Land Lost due to Submergence (km^2) for a) 2000 to 2100 global average time series, b) 2050 average for all models and scenarios, & c) 2050 standard deviation across all models, & d) 2050 standard deviation across all scenarios.

4.3. People flooded (PF)

Estimates of the number of additional PF per year in coastal regions are shown in Figure 13. As with the estimates of CFPD (see section 4.1.), numbers of PF per year are very dependent on the future scenario of coastal population (Figure 13a). For the high, A2, scenario of coastal population change (red line on Figure 13a), the number of PF globally is projected to increase by 21 million per year by 2030, 55 million per year by 2050, and 370 million per year by 2100. For the low, B1, scenario (blue line on Figure 13a), the same projections are 18 million per year by 2030, 42 million by 2050, and 165 million by 2100.

As was noted for LLS, after 2040 the rate of rise in the global number of PF per year increases from ~10 million per decade for both population scenarios, to ~60 million per decade for the A2 population scenario and 25 million per decade for the B1 population scenario. As with estimates of LLS, this increase in trend is related to increases in the coastal land areas lost to flooding, rather than any change in the trend in coastal population.

Spatially, the populations most at risk to coastal flooding from sea level rise are located in south and south-east Asia, particularly Bangladesh, India, Pakistan, eastern China, and southern Indonesia (highlighted orange, red and black on Figures 13b and c). Other susceptible regions are noted along the east coast of Africa, southern tip of Chile and the Nile delta. By 2050, the populations most at risk are in the Bay of Bengal, where up to 2.5 million PF per year are estimated (with the A2 population scenario). As with CFPD, the largest uncertainties relate to the differences in populations between scenarios.

a) Global average People Flooded (thousands/year)

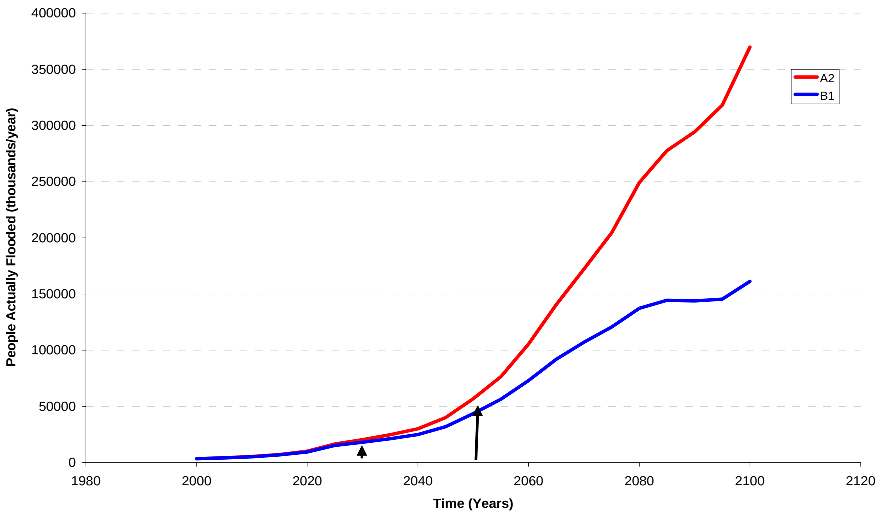

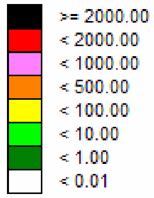

b) 2030 – People Flooded (thousands/year), A2 population

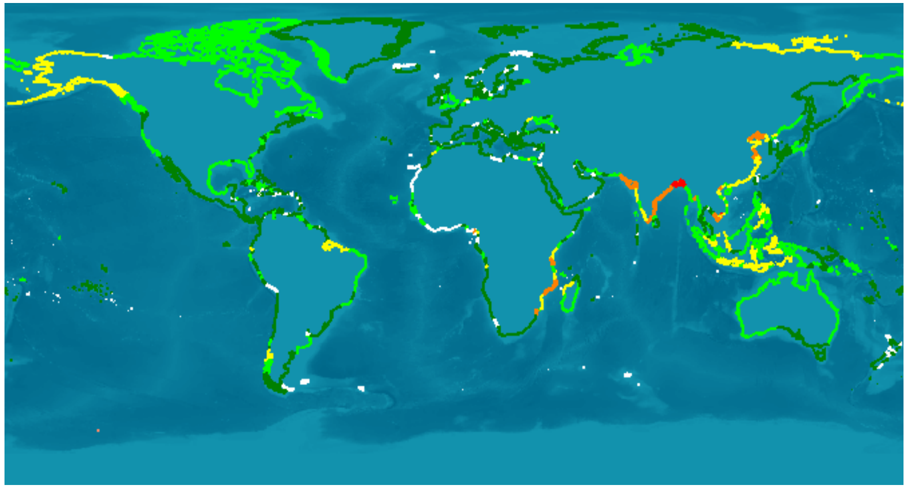

c) 2050 - People Flooded (thousands/year), A2 population

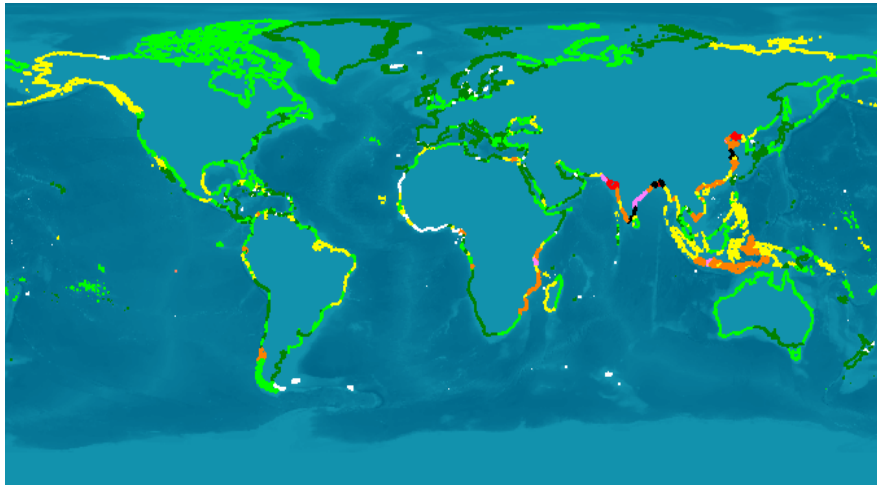

Figure 13. People Flooded (thousands/year) for a) 2000 to 2100 global average time series with population change according to the A2 and B1 SRES scenarios, b) 2030 average for all models and scenarios with A2 population, & c) 2030 average for all models and scenarios with A2 population.

References

Hinkel J 2005. DIVA – an iterative method for building modular integrated models. Advances in Geosciences, 4, 45-50.

IMAGE Team 2002. The IMAGE 2.2 implementation of the SRES scenarios, RIVM CD-ROM Publication 481508018, RIVM, Bilthoven.

IPCC 1998. The Regional Impacts of Climate Changes: An assessment of vulnerability. A Special Report of IPCC Working Group II. [Watson RT,Zinyowera MC, Moss RH (eds)]. Cambridge University Press, Cambridge, UK and New York. 517 pp.

IPCC 2000. Special Report on Emissions Scenarios: A Special Report of Working Group III of the Intergovernmental Panel on Climate Change. Cambridge University Press, Cambridge, UK and New York. 599pp.

IPCC 2001. Climate Change 2001: The Scientific Basis. Contribution of Working Group 1 to the Third Assessment Report ofd the Intergovernmental Panel on Climate Change [Houghton JT, Ding Y, Griggs DJ, Noguer M, van der Linden PJ, Dai X, Maskell K and Johnson CA (eds)]. Cambridge University Press, Cambridge, UK and New York. 881 pp.

McGill, J.T., 1958: Map of coastal landforms of the world. *Geographical Review*, 48, 402-405.

Nakicenovic, N. and Swart, R.J. 2001 IPCC Special Report on Emissions Scenarios. Cambridge: Cambridge University Press.

Peltier, W.R., 2000: Global glacial isostatic adjustment. In: *Sea-Level Rise: History and Consequences*, B.C. Douglas, M.S. Kearney and S.P. Leatherman (eds.), Academic Press, San Diego, CA, USA, 65–95.